A Model System for Developing a Tissue Engineered Meniscal Enthesis

Mary Clare McCorry[1], **Melissa M. Mansfield**[1], **Xiaozhou Sha**[1], **Daniel J. Coppola**[1], **Jonathan W. Lee**[1], **Lawrence J. Bonassar**[1,2,*]

Mary Clare McCorry: mcm338@cornell.edu; Melissa M. Mansfield: mmm449@cornell.edu; Xiaozhou Sha:
xs245@cornell.edu; Daniel J. Coppola: djc437@cornell.edu; Jonathan W. Lee: jwl287@cornell.edu

[1]Meinig School of Biomedical Engineering, 151 Weill Hall, Cornell University, Ithaca, NY 14853

[2]Sibley School of Mechanical and Aerospace Engineering, Cornell University, Ithaca, NY

Abstract

The meniscus acts as a stabilizer, lubricator, and load distributer in the knee joint. The mechanical stability of the meniscus depends on its connection to the underlying bone by a fibrocartilage to bone transition zone called the meniscal enthesis. Tissue engineered menisci hold great promise as a treatment alternative however lack a means of integrated fixation to the underlying bone needed in order for a tissue engineered meniscal replacement to be successful. Tissue engineering the meniscal enthesis is a difficult task given the complex gradients of cell type, mineral, and extracellular matrix molecules. Therefore there is a need for a simplified and high throughput enthesis model to test experimental parameters. The goal of this study was to develop a simplified enthesis model to test collagen integration with decellularized bone. We found that injection molding collagen into tubing loaded with decellularized bone plugs results in a scaffold with three regions: bone, bone-collagen, and collagen. Furthermore, collagen formation was directed in the axial direction using mechanical fixation at the bony ends. The results of this study show that this technique can be used to mimic the native enthesis morphology and serves as ideal test platform to generate a model tissue engineered enthesis.

GRAPHICAL ABSTRACT

*Address Correspondence to: Lawrence J. Bonassar, PhD., Professor, Meinig School of Biomedical Engineering, 149 Weill Hall, Cornell University, Ithaca, NY 14853, (607) 255-9381, lb244@cornell.edu.
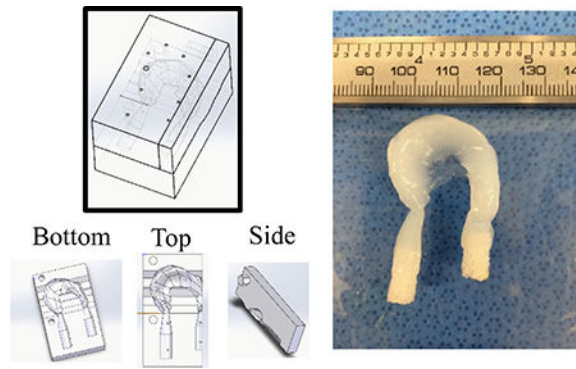
Keywords

Enthesis; Meniscus; Integration; Collagen Gel; Collagen Fibers

Introduction

The meniscus is a fibrocartilaginous structure in the knee that plays an essential role in the biomechanics and lubrication of the knee [1]. Loss or damage of the meniscus increases contact pressures within the knee and is known to lead to osteoarthritis [2,3]. Since natural healing of the meniscus is limited, current treatment options are partial meniscectomy, surgical repair, or meniscal allograft [4]. Other promising treatment options include artificial replacements, such as Actifit® and Menaflex™ collagen meniscus implant, and tissue engineered menisci [5,6].

A significant amount of work has been done on meniscus tissue engineering. Multiple reported approaches include using poly(ε-caprolactone) fibers seeded with encapsulated growth factors [7], biodegradable polyglycolic acid scaffold [8], and scaffold free self-assembly [9] to tissue engineer the meniscus. We have developed a cellular collagen based construct that is anatomically accurate including ligamentous extensions from the horns [10,11]. Additionally, we used mechanical fixation to anchor the tissue engineered meniscus at the horns to guide anisotropic fiber formation which improved mechanical and biochemical properties of the tissue engineered menisci [12]. Tissue engineered approaches have focused on the main body of the meniscus or simply aimed at a partial replacement. Proper fixation and restoration of the meniscal enthesis is necessary for long term success of a replacement. Tissue engineered menisci have shown great promise, however these methods are limited to partial meniscal replacement since they lack a soft tissue to bone enthesis for meniscal horn fixation.

The meniscus is attached to underlying bone at the meniscal horns by the meniscal entheses. The meniscal enthesis is a highly complex structure that consists of a gradient from fibrocartilage to bone tissue and provides mechanical fixation from a tensile loading environment to a compressive loading environment [13]. The meniscus to bone enthesis has four distinct regions: the ligamentious zone, uncalcified fibrocartilage, calcified fibrocartilage, and bone [14,15]. The ligamentous zone contains primarily fibroblasts and highly aligned collagen type I. The uncalcified fibrocartilage zone consists of

fibrochondrocytes (FCCs), chondrocytes, unaligned collagen type II, and proteoglycans. The calcified fibrocartilage contains hypertrophic chondrocytes and collagen types II and X. The bone region contains osteoblast, osteoclasts, osteocytes and collagen type I. These structures in combination are crucial to the mechanical performance of the meniscus [13,16]. Studies comparing allograft fixation methods have shown preserving the native enthesis and anchoring bone to bone is more successful over soft tissue to bone [17]. These methods provide a template for successful integration of tissue engineered menisci, however, methods for producing a tissue engineered meniscal enthesis have not been established.

The meniscal enthesis is a complex structure that is difficult to replicate *in vitro*. There are no published works on tissue engineering the meniscus to bone enthesis, however several groups have done work on tissue engineering the tendon- and ligament- to bone enthesis. Tendon, ligament, cartilage, and meniscal transitions to bone have similar complexities in structure since all three entheses transition from soft tissue to bone with complex gradients of extracellular matrix and cells [18]. Multiphasic scaffolds that use cell type, material, and chemical gradients are a common approach to tissue engineering the soft tissue to bone transition. Efforts to tissue engineer the ligamentous enthesis have used synthetic materials that are then seeded with coculture cell gradients [19–21], while other approaches utilize cellular matrix production to generate constructs from cell monolayers [22–24]. Osteochondral studies have developed bioreactor models that utilize diffusion systems to establish mineralization gradients in hydrogels [25,26]. While the meniscal enthesis has structural similarities to bone transition zones of ligament, tendon, and cartilage, there are distinct aspects to the meniscal attachment that necessitate a unique design approach for this interface.

Notably the fibers extend at an angle from the meniscus into underlying bone, unlike ligament and tendon where the fiber direction is consistent across the interface. Fibers from the meniscus interdigitated into the underlying bone are essential to the biomechanical performance of the meniscus [13,27]. However, little focus has been directed at replicating the integration of collagen fibers at the interface. Furthermore the meniscus has a unique cell type, fibrochondrocytes, whose behavior at such interfaces has not yet been characterized. Collagen type I gels are a common scaffold material used in tissue engineering and local fiber organization can be guided by static mechanical boundary condition such as clamping [28]. We hypothesize that integrated fiber formation can be guided by applying a mechanical boundary condition to a multiphasic scaffold using decellularized bone plugs and collagen.

The meniscal enthesis is a complex tissue and methods to generate an integrated tissue construct with a soft to hard transition is not well understood. The overarching goal of this project is to develop an experimental platform to study integration of meniscus tissue with bone. Such a platform would enable targeted experiments on the effect chemical and mechanical signals that affect cellular behavior in the meniscal enthesis. The specific goal of this study was to examine the integration of FCC seeded collagen gels to decellularized bone and determine the effect of clamping on the organization of collagen at the soft tissue to bone interface.

Materials and Methods

Bone Plug Extraction

Trabecular bone plugs were extracted from the distal femur of 1–3 day old bovids using a 6 mm diameter coring bit. Bone cores were sectioned into 10 mm long cylinders that were then decellularized in order to remove cellular debris while maintaining trabecular scaffold material and shape (Figure 2A). Bone plugs were rinsed of all marrow and debris using a stream of high velocity deionized water. Plugs were then washed in a solution of phosphate buffered saline (PBS) with 0.1% ethylenediaminetetraacetic acid (EDTA) (wt/vol%) and placed on shaker at room temperature. Following the washes, bone plugs were put in a hypotonic buffer (10mM Trizma base, 0.1% EDTA (wt/vol%) and soaked for at least 24 hours at 4°C. Bone plugs were soaked in a detergent comprised of 10mM Trizma base and 0.5% sodium dodecyl sulfate (SDS) (wt/vol%) for 24 hours at room temperature on a shaker to remove cellular debris. Decellularization of samples was confirmed by staining histological samples with hematoxylin (Supplemental 2). Bone plugs demineralized using a similar protocol have been shown to be viable scaffold for tissue engineering bone [29,30]. Following washes with PBS, samples were frozen for later use. Prior to experimental use, bone plugs were lyophilized and soaked in ethanol for 2 hours, rinsed with PBS, and then soaked in Dulbecco's modified Eagle's medium (DMEM).

Construct Generation

Constructs were comprised of decellularized bone plugs, high density collagen type I, and FCCs (Supplementary Video 1). Collagen was extracted from Sprague-Dawley rat tails (Pel-Freez Biologicals, Rogers, AZ) as previously described [10,31]. Briefly, rat tail tendons were purified and dissolved in 0.1% acetic acid at a stock concentration of 30 mg/mL stored at 4°C. FCCs were obtained from the menisci of 1–3 day old bovids as previously described [10,32]. Menisci were digested in 0.3% collagenase (Worthington Biochemical Corporation, Lakewood, NJ) dissolved in DMEM for 16–18 hours. The collagenase solution was then filtered through a 100 μm strainer and cells were centrifuged and washed with PBS and suspended in DMEM.

Anatomically accurate tissue engineered menisci terminating in bone where generated by modifying previously designed meniscus molds. Previously designed anatomically accurate meniscus molds were modified to contain the trabecular bone plugs (Figure 1) [11,12]. Molds were 3D printed with injection molding ports. Bone plugs were preloaded into the molds and high density collagen was injected into molds resulting in a tissue engineered construct with bony inserts. These constructs contained a large amount of material far from the bone to soft tissue interface that would require a significant amount of collagen and FCCs to generate. Therefore, a simplified linear design was used to streamline testing to optimize the collagen to bone interface (Figure 2).

Enthesis constructs were produced by inserting decellularized bone plugs 20 mm apart into Tygon® tubing (Figure 2B). Bone plugs were prevented from moving backwards during injection molding by adding binder clips to either end (Figure 2B). Small holes were placed at both ends of the tube to direct air flow and in the center for the injection needle. To start

the collagen gelation process the stock collagen was returned to a neutral 7.0 pH and 300mOsm by mixing with a working solution of 1N NaOH, 10× PBS, and 1× PBS. This solution immediately mixed with a cellular media of FCCs for a final concentration of 20 mg/mL collagen and 25×10^6 cells/mL. The collagen and cells mixture was then injection molded into the center hole in the Tygon® tubing (Figure 2C). Constructs were then placed in an incubator at 37°C for 45 minutes to complete gelation process. Following incubation, constructs were removed from the Tygon® molding and placed either in a custom machined polysulphone mold for clamping or in a 55 mm^2 petri dish (Figure 3A). Constructs placed in the polysulphone mold were clamped into culture troughs 12 hours after construct formation using stainless steel clamps at the bony portion of the constructs. Samples were cultured for 0, 2, and 4 weeks in media containing DMEM, 10% FBS, 100 μg/mL penicillin, 100 μg/mL streptomycin, 0.1 mM non-essential amino acids, 50 μg/mL ascorbate, and 0.4 mM L-proline [10,11]. A total of 10 samples were processed per group with 8 samples tracked for contraction, 6 tensile tested, and 4 embedded in paraffin for histological analysis.

Histology

At the conclusion of each culture period, constructs were fixed in 10% buffered formalin for 24–48 hours, demineralized, dehydrated, and embedded in paraffin. Sections of enthesis constructs were cut longitudinally and stained with Masson's trichrome and Picrosirius red. Picrosirius red staining was imaged using both brightfield microscopy and polarized light to illuminate collagen fibers. Histological stains were viewed using a Nikon Eclipse TE2000-S microscope (Nikon Instruments, Melville, NY) and images taken using a SPOT RT camera (Diagnostic Instruments, Steriling Heights, MI) attached to the microscope.

Tensile Testing

Constructs underwent tensile testing using an Enduratec ElectroForce 3200 System (Bose, Eden Prairie, MN) using a 250 g load cell [11]. A 0.75%/sec strain rate was applied to mimic quasistatic loading. Samples were clamped at bone attachments and length was calculated as the distance between the bone to collagen interfaces. The elastic modulus and ultimate tensile strength (UTS) of the constructs were calculated from the measured stress and strain curves (Supplemental 3). The elastic modulus was measured as the slope of the linear elastic region of the stress vs strain curve ($E_{Elastic}$). The UTS was the maximum stress value that the constructs withstood before failure. A second modulus was calculated from the linear portion in the toe region (E_{Toe}). A transition strain (ε_{Trans}) was calculated at the intersection of the linear fits for $E_{Elastic}$ and E_{Toe}.

Contraction Analysis

Images of the constructs were taken every 3–4 days during media changes. The length, width and area of the constructs were measured using ImageJ [33] and then compared to the length, width and area measured at day 0, to calculate the percent contraction at each day. Length was measured as the distance between the inner edges of bone plugs. Width was measured as the diameter at the center of the construct. Since width varied across the length of the construct, the area of the collagen portion of the construct was measured by outlining the area by hand.

Statistics

All data were analyzed using a 2-way ANOVA with Tukey's post hoc analysis (SigmaPlot, San Jose, California). Data points were graphed with mean ±SD and significance was determined with $p < 0.05$.

Results

Construct Generation

Tissue engineered enthesis constructs were assembled in a simple manner that created regions of bone and collagen with a distinct interface (Figure 2C). Bone was decellularized, while regions containing collagen were seeded with FCCs throughout the collagen material. Following injection and gelation of collagen, constructs were robust enough for physical handling and manipulation. Collagen penetrated ~3–5mm into the bone plugs on either end, creating an interface region between the bone region and collagen region (Figure 2D). Constructs were easily removed from the Tygon® tubing mold and placed in clamping plates to be cultured for up to 4 weeks (Figure 3A). Distinct changes in collagen contraction occurred as a result of clamping condition. Clamping greatly affected construct morphology with unclamped samples significantly contracting in length, width, and projected area over 4 weeks ($p < 0.05$ for all measurements) (Figure 3B-E). In contrast, clamped samples maintained 65–75% of initial dimensions over four weeks (Figure 3C-E).

Histological Morphology

Apparent morphological similarities between native enthesis and the tissue engineered meniscal enthesis were apparent in Picrosirius red histology (Figure 4). The structure of individual trabeculae obtained from decellularized bone have the same morphological organization seen in the native enthesis bone region. Collagen penetrated into the pores between trabeculae at the start of culture, and remained throughout the 4 weeks of culture in both unclamped and clamped samples (Figure 4).

Clamping samples during culture induced the formation of large longitudinally oriented fiber bundles (Figure 5). At 0 weeks constructs had small disorganized fibers. Unclamped samples developed radially aligned fibers that were parallel to the interface bone edge interface. In the body and at the radial edge of the collagen region fibers were smaller and less prominent, but generally still organized parallel to the bone interface. Clamped samples formed fibers mainly along the longitudinal axis of the collagen cylinder. Longitudinal fibers were consistently seen along the outer edge of the collagen cylinder, however fibers were less organized near the center.

In regions of organized fiber bundles, cells were elongated in the direction of fibers while in regions of less organized collagen, cells were more rounded (Figure 6). Cells in the 0 week constructs were uniformly distributed throughout the collagen. Cells in all three regions appeared rounded within the collagen scaffold. After four weeks of culture, cells remained embedded within the collagen and did not migrate onto the bone matrix scaffold. Cells in the bony region appear rounded, whereas cells in the interface and collagen body are a mix of elongated and rounded cells. Cells elongate in the direction of collagen fibers. In the

unclamped samples the cells elongated in the radial direction, whereas the cells in the clamped samples elongate more in the longitudinal direction.

Mechanical Properties

Clamping condition increased mechanical properties of constructs over 4 weeks in culture (Figure 7). The elastic modulus significantly increased after 2 and 4 weeks of culture, increasing 500% after 4 weeks under clamped condition compared to the 0 week start point (Figure 7A, $p < 0.05$). Unclamped samples only increased by 150% after 4 weeks (Figure 7A, $p < 0.05$). UTS followed a similar trend with significant increases after 4 weeks in culture, increasing 400% with the clamped condition and 250% with the unclamped condition over the 4 week culture period (Figure 7B, $p < 0.05$). The modulus in the toe region similarly increased with time in culture with clamped samples transitioning out of the toe region into the elastic region at a lower transition strain (Supplemental 4). While the midsubstance of collagen is strengthened over time and condition, ultimate failure location changed accordingly. The 0 week and 2 week unclamped samples' predominant failure location was in the midsubstance of the collagen. The 2 week clamped and both 4 week clamped and unclamped conditions resulted in failure primarily at the collagen to bone interface.

Discussion

The objective of this study was to develop an experimental test platform for tissue engineering the meniscal enthesis. A major challenge in attaching tissue engineered menisci *in vivo* is anchoring soft tissue to bone, which points to developing soft constructs seeded with FCCs that interface with bone. Here we demonstrated that FCC seeded collagen integrates into decellularized bone plugs producing a mechanically robust interface that can be cultured. Anchoring at the bone (clamping) enhances the formation of tissue with regards to fiber formation and cellular organization. Anchored samples formed fibers in the longitudinal direction which maintained construct morphology and improved mechanical properties.

A collagen injection molding technique established three distinct regions that further developed throughout culture: 1) bone, 2) bone-collagen interface, and 3) collagen. Each region had a distinct material composition and structure. The bony region contained the decellularized bone matrix material which is an excellent template for mineral formation and matrix development [34]. Decellularized bone matrix maintains the native architecture and mechanical properties of bone [35]. Additionally, bone matrix is known to contain critical biological factors and microtopography that increase the osteoinductive properties of the scaffold and in turn improves bone formation [36]. Furthermore, the decellularization process used in this study has been proven amenable to cellular reseeding and new bone development in pre-clinical studies[29,30]. Attaching the meniscus through a bone plug will likely improve implant integration with native bone [17]. Collagen type I was chosen for the soft tissue portion of constructs because it is the major structural protein in the meniscus and ligament and has been used as a scaffold for regeneration of these tissues in many studies [18,37–39]. Further, collagen type I is unique in that the matrix can be remodeled to form large mature fiber networks [28]. The bone-collagen interface region was formed by

infiltrating the pores of decellularized bone with FCC seeded collagen. This infiltration enabled directed mechanical anchoring of the soft collagen to bone as well as cell-mediated reorganization of this region (Figures 3 and 4). The infiltration of large fibers extending from the meniscal horns into the uncalcified cartilage region of the native meniscal enthesis is essential the mechanical integrity of the construct [13,40]. Therefore, the integration of collagen with bone at the interface will be important for transitioning mechanical strains in the tissue engineered enthesis.

Mechanical fixation guided cellular behavior to drive organized fiber formation. After four weeks of culture, the matrix which was disorganized at 0 weeks contained larger and more organized fibers. The specific organization of fibers depended on the absence or presence of mechanical fixation. Unclamped samples contracted along the longitudinal axis bringing the bony ends closer together and forming fibers in the radial direction. In contrast, clamped samples maintained original length and formed fibers in the longitudinal direction between bony ends. Furthermore, clamped samples had continuous fibers that spanned the collagen and bone regions. As the construct contracted in unclamped samples radial fibers compacted at the bony interface rather than longitudinally integrating like the anchored samples. Stacking of radial fibers at the interface was analogous to the folding of an accordion. The native enthesis contains a dense network of collagen fibrils primarily in the longitudinal direction [14,40]. The longitudinal fibers in the clamped samples are more representative of the native collagen orientation.

The reorganization of fibers based on mechanical boundary conditions is consistent with several studies of cell based remodeling with collagen [12,28,41,42]. This phenomenon has been noted across several cell types including dermal fibroblasts [41], cardiomyocytes [28], annulus fibrosis chondrocytes [42], and meniscal fibrochondrocytes [12]. Previous studies in whole meniscus tissue engineering showed that FCCs can remodel collagen into organized fibers guided by mechanical fixation [12]. Furthermore, guided collagen reorganization in this study resembles that seen in native meniscus during development. The meniscus begins as a dense mesenchymal condensate and the development of organized fibers is not observed until after meniscal attachments to the tibia are established [43–46]. Similarly in this study, we begin with a high density of cells embedded in a collagen matrix that is then mechanically anchored to induce organized fiber development over time. Further mechanical and chemical stimulation will be required to further develop this tissue, however the system used in this study will serve as a useful model for meniscal enthesis development.

Integration between scaffold regions is paramount to the mechanical performance of hard to soft tissue interfaces. *In vivo* the meniscal enthesis assists in the transition from the tensile loading environment of the meniscus into the underlying compressive loading environment of bone [47,48]. The meniscal enthesis must be able to withstand high tensile loads [49,50]. Native stiffness and UTS range from approximately 125–300 MPa and 5–75MPa respectively [50,51]. Although we have yet to achieve native UTS and stiffness, this study shows that we are able use mechanical fixation to improve mechanical performance under tensile loads provided by cellular traction forces. The increase in mechanical properties is likely do to local matrix reorganization of fibers in the direction of load as well as increased integration at the bony interface. Since most mechanical failures occurred at the interface,

the measurements reported are not a true measure of the bulk collagen properties. The lack of mechanical property accrual between 2 and 4 weeks of culture is likely due to a lack of increased mechanical integration at the interface. While the constructs do not meet the criteria for a fully functional bone-meniscus interface, constructs do develop a bone-soft tissue interface with a continuous collagen matrix that spans the interface with interconnecting fibers. In vivo studies in a tissue engineered ligament have shown the development of integrated fibers to bone that performed well under tensile load after 6 months in vivo [24]. However, development of interconnecting fibers in vitro at the interface has yet to be demonstrated in enthesis tissue engineering. This simplified in vitro system provides a platform for screening methods to enhance the structure and properties of this interface that contribute to mechanical performance.

The simplicity of this model is easily transferable to address several different experimental questions. Previously we designed a tissue engineered meniscus [11,12,52], this meniscus can be combined with the linear model design used in this study to translate into a full scale tissue engineered meniscus (Figure 1). We have shown in this the study the application of mechanical constraint to influence fiber formation, however this system can easily be utilized as a model system to test experimental parameters for tissue engineering the meniscus to bone enthesis. The culture set up was further optimized for high throughput testing. Polysulphone molds were redesigned and expanded to clamp a capacity of six constructs with a media wall for future experiments (Supplemental 1). Other efforts to engineer hard to soft interfaces as a model system involve creating media gradients using multi-media chamber bioreactors. The Tuan group recently developed a dual-chamber bioreactor for tissue specific media culture of an osteochondral junction [53], while a different group used a double diffusion system to create a target zone of calcification [25]. The diffusion systems focus on creating chemical gradients, while our stem uses boundary conditions to direct fiber formation into the porous bone. Our design has been simplified to serve as a test to investigate a host of experimental parameters such as the application of different cell types in co-culture, biochemical gradients, and demineralization gradients. Using a streamlined culture system for optimization will improve the ultimate application to a tissue engineered meniscus design.

The construct designed in this study was primarily engineered to serve as a simplified model for testing tissue engineering considerations when creating the meniscal enthesis *in vitro.* Given that this is a simplified model, the setup has some limitations, notably in the mechanical properties and in the lack of a calcified cartilage layer. Further studies on fabrication and culture technique may enable development of more functionally organized tissues. Additionally, our construct is a linear structure where the bones on each end are linear and level with each other. Native entheses fibrocartilage to bone transitions are at an angle to the ligamentous fiber direction, additionally this angle will vary depending on the specific enthesis. Meniscal entheses have been shown to each have their own unique mechanical properties and anatomy, which presents a challenge to a one-size-fits-all tissue engineering approach [54,55]. Although the constructs generated in this study showed improvement in mechanical properties, the constructs were still well below native properties. This study only investigated clamping as an approach to improve mechanical properties. Other approaches such as collagen crosslinking, growth factors, and mineral gradients have

shown success in other studies and could easily be applied to our experimental set up to improve mechanical properties [25,56–58]. Future studies could benefit from the addition of enthesis specific cells in tissue engineered enthesis region. These constructs did not see the development of a tidemark, likely due to the lack of FCC motility and short culture duration. Future work will focus on the addition of cells directly to bone constructs and increase culture duration. Ideally a tissue engineered meniscal enthesis could continue to remodel once implanted *in vivo* to better suit the unique mechanical loads in that specific location.

Conclusions

This study demonstrated that collagen and bone can be integrated together into a simplified test model for meniscus-to-bone tissue engineering. Furthermore, we showed that collagen alignment can be directed to integrate with bone using mechanical clamping. Collagen infiltration into bone pores at the collagen-bone interface facilitates the directed integration of fibers at the interface. This experimental model of the bone-fibrocartilage interface serves as a platform to better understand the interaction between these two very different tissues and to provide a platform for screen methods to enhance the structure and properties of this interface.

Supplementary Material

Refer to Web version on PubMed Central for supplementary material.

Acknowledgements

References

[1]. Makris E, Hadidi P, Athanasiou K, The knee meniscus: structure-function, pathophysiology, current repair techniques, and prospects for regeneration., Biomaterials. 32 (2011) 7411–31. [PubMed: 21764438]

[2]. Bedi A, Kelly NH, Baad M, Fox AJS, Brophy RH, Maher RFSA, Dynamic contact mechanics of the medial meniscus as a function of radial tear, repair, and partial meniscectomy., J. Bone Joint Surg. Am 92 (2010) 1398–1408. [PubMed: 20516315]

[3]. McDermott ID, Amis AA, The consequences of meniscectomy., J. Bone Joint Surg. Br 88 (2006) 1549–1556. [PubMed: 17159163]

[4]. Hutchinson ID, Moran CJ, Potter HG, Warren RF, Rodeo SA, Restoration of the meniscus: form and function., Am. J. Sports Med 42 (2014) 987–98. [PubMed: 23940202]

[5]. Martinek V, Ueblacker P, Bräun K, Nitschke S, Mannhardt R, Specht K, Gansbacher B, Imhoff AB, Second generation of meniscus transplantation: in-vivo study with tissue engineered meniscus replacement., Arch. Orthop. Trauma Surg 126 (2006) 228–34. [PubMed: 16215722]

[6]. Moran CJ, Orth F, Withers DP, Orth F, Kurzweil PR, Verdonk PC, Clinical Application of Scaffolds for Partial Meniscus Replacement, 23 (2015) 156–161.

[7]. Lee CH, Rodeo SA, Fortier LA, Lu C, Erisken C, Mao JJ, Protein-releasing polymeric scaffolds induce fibrochondrocytic differentiation of endogenous cells for knee meniscus regeneration in sheep, 6 (2014) 1–12.

[8]. Kang S, Son S, Lee J, Lee E, Lee K, Park S, Park J, Kim B, Regeneration of whole meniscus using meniscal cells and polymer scaffolds in a rabbit total meniscectomy model, (2006) 7–11.

[9]. Aufderheide AC, a Athanasiou K, Assessment of a bovine co-culture, scaffold-free method for growing meniscus-shaped constructs., Tissue Eng. 13 (2007) 2195–205. [PubMed: 17630876]

[10]. Puetzer JL, Bonassar LJ, High Density Type I Collagen Gels for Tissue Engineering of Whole Menisci., Acta Biomater. 9 (2013) 7787–7795. [PubMed: 23669622]

[11]. Ballyns JJ, Gleghorn JP, Niebrzydowski V, Rawlinson JJ, Potter HG, Maher SA, Wright TM, Bonassar LJ, Image-guided tissue engineering of anatomically shaped implants via MRI and micro-CT using injection molding., Tissue Eng. Part A 14 (2008) 1195–202. [PubMed: 18593357]

[12]. Puetzer JL, Koo E, Bonassar LJ, Induction of fiber alignment and mechanical anisotropy in tissue engineered menisci with mechanical anchoring, J. Biomech 48 (2015) 1436–1443. [PubMed: 25770753]

[13]. Abraham AC, Haut Donahue TL, From meniscus to bone: A quantitative evaluation of structure and function of the human meniscal attachments, Acta Biomater. 9 (2013) 6322–6329. [PubMed: 23385217]

[14]. Villegas DF, Hansen T. a., Liu DF, Donahue T.L. Haut, A quantitative study of the microstructure and biochemistry of the medial meniscal horn attachments, Ann. Biomed. Eng 36 (2008) 123–131. [PubMed: 17999192]

[15]. Gao J, Immunolocalization of types I, II, and X collagen in the tibial insertion sites of the medial meniscus., Knee Surg. Sports Traumatol. Arthrosc 8 (2000) 61–65. [PubMed: 10663323]

[16]. Haut Donahue TL, Hull ML, Rashid MM, Jacobs CR, How the stiffness of meniscal attachments and meniscal material properties affect tibio-femoral contact pressure computed using a validated finite element model of the human knee joint, J. Biomech 36 (2003) 19–34. [PubMed: 12485635]

[17]. Wang H, Gee AO, Hutchinson ID, Stoner K, Warren RF, Chen TO, Maher SA, Bone Plug Versus Suture-Only Fixation of Meniscal Grafts: Effect on Joint Contact Mechanics During Simulated Gait., Am. J. Sports Med (2014).

[18]. Yang PJ, Temenoff JS, Engineering orthopedic tissue interfaces., Tissue Eng. Part B. Rev 15 (2009) 127–41. [PubMed: 19231983]

[19]. Spalazzi JP, Doty SB, Moffat KL, Levine WN, Lu HH, Development of controlled matrix heterogeneity on a triphasic scaffold for orthopedic interface tissue engineering., Tissue Eng. 12 (2006) 3497–508. [PubMed: 17518686]

[20]. Spalazzi JP, Dagher E, Doty SB, Guo XE, a Rodeo S, Lu HH, In vivo evaluation of a multiphased scaffold designed for orthopaedic interface tissue engineering and soft tissue-to-bone integration., J. Biomed. Mater. Res. A 86 (2008) 1–12. [PubMed: 18442111]

[21]. Criscenti G, Longoni A, Di Luca A, De Maria C, Van Blitterswijk CA, Vozzi G, Moroni L, Triphasic scaffolds for the regeneration of the bone–ligament interface, Biofabrication. 8 (2016) 15009.

[22]. Mahalingam VD, Behbahani-Nejad N, Ronan EA, Olsen TJ, Smietana MJ, Wojtys EM, Wellik DM, Arruda EM, Larkin LM, Fresh versus frozen engineered bone-ligament-bone grafts for sheep anterior cruciate ligament repair., Tissue Eng. Part C. Methods 21 (2015) 548–56. [PubMed: 25397990]

[23]. Mahalingam VD, Behbahani-Nejad N, V Horine S, Olsen TJ, Smietana MJ, Wojtys EM, Wellik DM, Arruda EM, Larkin LM, Allogeneic versus autologous derived cell sources for use in engineered bone-ligament-bone grafts in sheep anterior cruciate ligament repair., Tissue Eng. Part A Part A 21 (2015) 1047–54.

[24]. Ma J, Smietana MJ, Kostrominova TY, Wojtys EM, Larkin LM, Arruda EM, Three-Dimensional Engineered Bone–Ligament–Bone Constructs for Anterior Cruciate Ligament Replacement, Tissue Eng. Part A 18 (2012) 103–116. [PubMed: 21902608]

[25]. Hollenstein J, Terrier A, Cory E, Chen AC, Sah RL, Pioletti DP, Mechanical evaluation of a tissue-engineered zone of calcification in a bone-hydrogel osteochondral construct., Comput. Methods Biomech. Biomed. Engin 18 (2013) 37–41.

[26]. Lozito TP, Alexander PG, Lin H, Gottardi R, Cheng AW-M, Tuan RS, Three-dimensional osteochondral microtissue to model pathogenesis of osteoarthritis., Stem Cell Res. Ther 4 Suppl 1 (2013) S6. [PubMed: 24564995]

[27]. Chen MI, Branch TP, Hutton WC, Is it important to secure the horns during lateral meniscal transplantation? A cadaveric study., Arthroscopy. 12 (1996) 174–181. [PubMed: 8776994]

[28]. Costa KD, Lee EJ, Holmes JW, Creating alignment and anisotropy in engineered heart tissue: role of boundary conditions in a model three-dimensional culture system., Tissue Eng. 9 (2003) 567–77. [PubMed: 13678436]

[29]. Grayson WL, Fröhlich M, Yeager K, Bhumiratana S, Chan ME, Cannizzaro C, Wan LQ, Liu XS, Guo XE, Vunjak-Novakovic G, Engineering anatomically shaped human bone grafts., Proc. Natl. Acad. Sci. U. S. A 107 (2010) 3299–3304. [PubMed: 19820164]

[30]. Grayson WL, Bhumiratana S, Cannizzaro C, Chao P-HG, Lennon DP, Caplan AI, Vunjak-Novakovic G, Effects of initial seeding density and fluid perfusion rate on formation of tissue-engineered bone., Tissue Eng. Part A 14 (2008) 1809–20. [PubMed: 18620487]

[31]. Cross VL, Zheng Y, Won Choi N, Verbridge SS, Sutermaster B. a., Bonassar LJ, Fischbach C, Stroock AD, Dense type I collagen matrices that support cellular remodeling and microfabrication for studies of tumor angiogenesis and vasculogenesis in vitro, Biomaterials. 31 (2010) 8596–8607. [PubMed: 20727585]

[32]. Mauck RL, Yuan X, Tuan RS, Chondrogenic differentiation and functional maturation of bovine mesenchymal stem cells in long-term agarose culture., Osteoarthr. Cartil 14 (2006) 179–89. [PubMed: 16257243]

[33]. Abràmoff MD, Magalhães PJ, Ram SJ, Image processing with imageJ, Biophotonics Int. 11 (2004) 36–41.

[34]. Reddi AH, Morphogenetic messages are in the extracellular matrix: biotechnology from bench to bedside, Biochem. Soc. Trans 28 (2000) 345–349. [PubMed: 10961916]

[35]. Gilbert TW, Sellaro TL, Badylak SF, Decellularization of tissues and organs, Biomaterials. 27 (2006) 3675–3683. [PubMed: 16519932]

[36]. Papadimitropoulos A, Scotti C, Bourgine P, Scherberich A, Martin I, Engineered decellularized matrices to instruct bone regeneration processes, Bone. 70 (2015) 66–72. [PubMed: 25260931]

[37]. Oda S, Otsuki S, Kurokawa Y, Hoshiyama Y, Nakajima M, Neo M, A new method for meniscus repair using type I collagen scaffold and infrapatellar fat pad, J. Biomater. Appl 0 (2015) 1–10.

[38]. Pabbruwe MB, Kafienah W, Tarlton JF, Mistry S, Fox DJ, Hollander AP, Repair of meniscal cartilage white zone tears using a stem cell/collagen-scaffold implant., Biomaterials. 31 (2010) 2583–91. [PubMed: 20053438]

[39]. Hansen R, Bryk E, Vigorita V, Collagen scaffold meniscus implant integration in a canine model: a histological analysis., J. Orthop. Res 31 (2013) 1914–9. [PubMed: 23939994]

[40]. Villegas DF, Donahue TLH, Collagen morphology in human meniscal attachments: a SEM study., Connect. Tissue Res 51 (2010) 327–336. [PubMed: 20388017]

[41]. Grinnell F, Fibroblast-collagen-matrix contraction: growth-factor signalling and mechanical loading, Trends Cell Biol. 10 (2000) 362–365. [PubMed: 10932093]

[42]. Bowles RD, Williams RM, Zipfel WR, Bonassar LJ, Self-Assembly of Aligned Tissue-Engineered Annulus fibrosus and Intervertebral Disc Composite Via Collagen Gel Contraction, Tissue Eng. Part A 16 (2010).

[43]. Clark CR, Ogden JA, Prenatal and Postnatal Development of Human Knee Joint Mensci, Iowa Orthop. J 1 (1981) 20–27.

[44]. a Mérida-Velasco J, Sánchez-Montesinos I, Espín-Ferra J, Rodríguez-Vázquez JF, Mérida-Velasco JR, Jiménez-Collado J, Development of the human knee joint., Anat. Rec 248 (1997) 269–78. [PubMed: 9185993]

[45]. Gray DJ, Gardner E, Prenatal development of the human knee and superior tibiofibular joints, Am. J. Anat 86 (1950) 235–287. [PubMed: 15410671]

[46]. Gardner E, O'Rahilly R, The early development of the knee joint in staged human embryos., J. Anat 102 (1968) 289–99. [PubMed: 5643844]

[47]. Seitz A, Kasisari R, Claes L, Ignatius A, Dürselen L, Forces acting on the anterior meniscotibial ligaments, Knee Surgery, Sport. Traumatol. Arthrosc 20 (2012) 1488–1495.

[48]. Stärke C, Kopf S, Gröbel KH, Becker R, Tensile forces at the porcine anterior meniscal horn attachment, J. Orthop. Res 27 (2009) 1619–1624. [PubMed: 19572411]

[49]. Masouros SD, McDermott ID, Amis AA, Bull a. M.J., Biomechanics of the meniscus-meniscal ligament construct of the knee, Knee Surgery, Sport. Traumatol. Arthrosc 16 (2008) 1121–1132.

[50]. Ellman MB, Laprade CM, Smith SD, Rasmussen MT, Engebretsen L, Wijdicks CA, LaPrade RF, Structural Properties of the Meniscal Roots., Am. J. Sports Med (2014) 1–7.

[51]. Villegas DF, Maes J. a., Magee SD, Donahue T.L. Haut, Failure properties and strain distribution analysis of meniscal attachments, J. Biomech 40 (2007) 2655–2662. [PubMed: 17359982]

[52]. Puetzer JL, Bonassar LJ, Physiologically Distributed Loading Patterns Drive the Formation of Zonally Organized Collagen Structures in Tissue Engineered Meniscus, Tissue Eng. Part A (2016) 1–40.

[53]. Alexander PG, Gottardi R, Lin H, Lozito TP, Tuan RS, Three-dimensional osteogenic and chondrogenic systems to model osteochondral physiology and degenerative joint diseases., Exp. Biol. Med. (Maywood). (2014) 1–16.

[54]. Hauch KN, Oyen ML, Odegard GM, Haut Donahue TL, Nanoindentation of the insertional zones of human meniscal attachments into underlying bone, J. Mech. Behav. Biomed. Mater 2 (2009) 339–347. [PubMed: 19627840]

[55]. Wang YJ, Yu JK, Luo H, Yu CL, Ao YF, Xie X, Jiang D, Zhang JY, An anatomical and histological study of human meniscal horn bony insertions and peri-meniscal attachments as a basis for meniscal transplantation, Chin. Med. J. (Engl). 122 (2009) 536–540. [PubMed: 19323904]

[56]. Pangborn CA, Athanasiou KA, Effects of growth factors on meniscal fibrochondrocytes., Tissue Eng. 11 (2005) 1141–8. [PubMed: 16144450]

[57]. Makris EA, Responte DJ, Paschos NK, Hu JC, Athanasiou KA, Developing functional musculoskeletal tissues through hypoxia and lysyl oxidase-induced collagen cross-linking, Proc. Natl. Acad. Sci 111 (2014) E4832–E4841. [PubMed: 25349395]

[58]. Roy R, Boskey AL, Bonassar LJ, Non-enzymatic glycation of chondrocyte-seeded collagen gels for cartilage tissue engineering, J. Orthop. Res 26 (2008) 1434–1439. [PubMed: 18473383]

Statement of Significance

The meniscal enthesis is a complex structure that is essential to mechanical stability of the meniscus and the knee joint. Several studies document the development of anatomically shaped tissue engineered meniscus constructs, but none have focused on how to integrate such tissues with underlying bone. This study establishes a simplified construct to model the meniscal enthesis composed of a collagen gels seeded with meniscal fibrochondrocytes integrated with decellularized cancellous bone. Mechanical fixation at the bony ends induced tissue integration of fibers into the bony tissue, which is critical for mechanical performance and has yet to be shown in enthesis literature. Our test platform is amenable to targeted experiments investigating mineralization gradients, collagen fiber alignment, cell population phenotype, and media conditioning with experimental impact on enthesis studies for meniscus, tendon, and ligament.
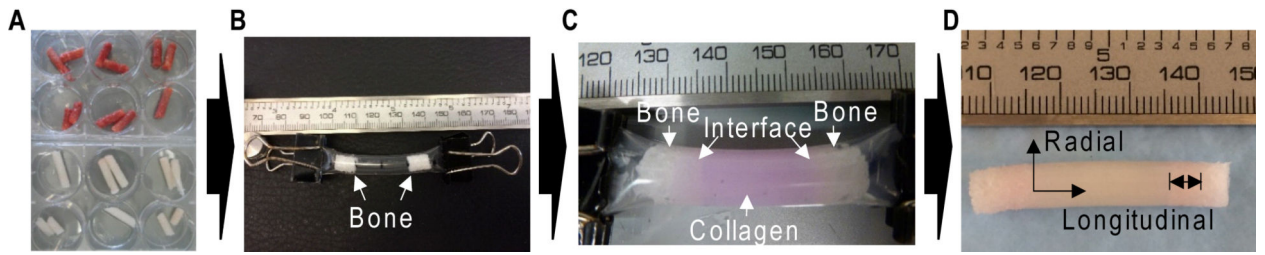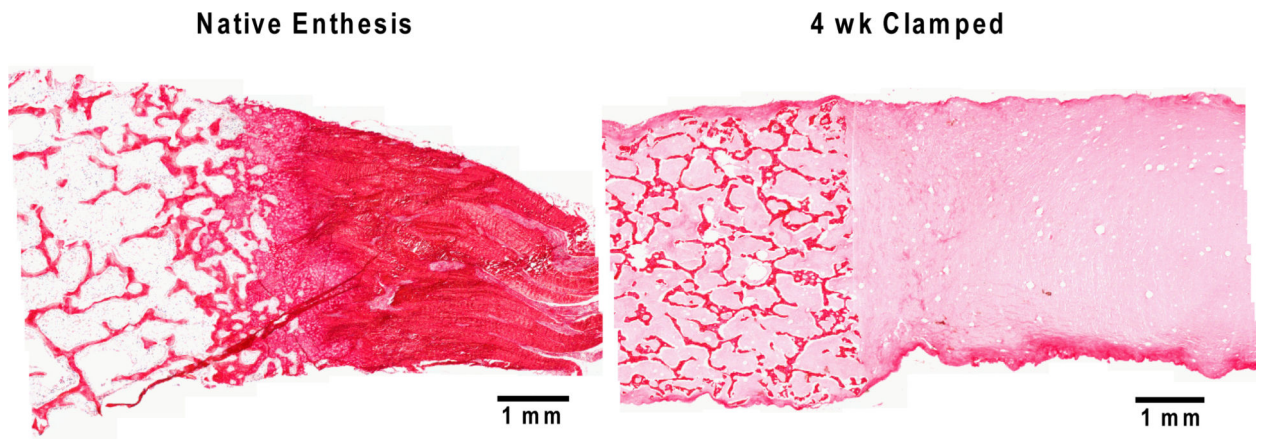
Figure 1:
Full tissue engineered meniscus with bone plug attachments. Injection mold design for full scale tissue engineered meniscus with enthesis attachments (left). Injection molded anatomically accurate tissue engineered meniscus with integrated bone plug entheses (left).
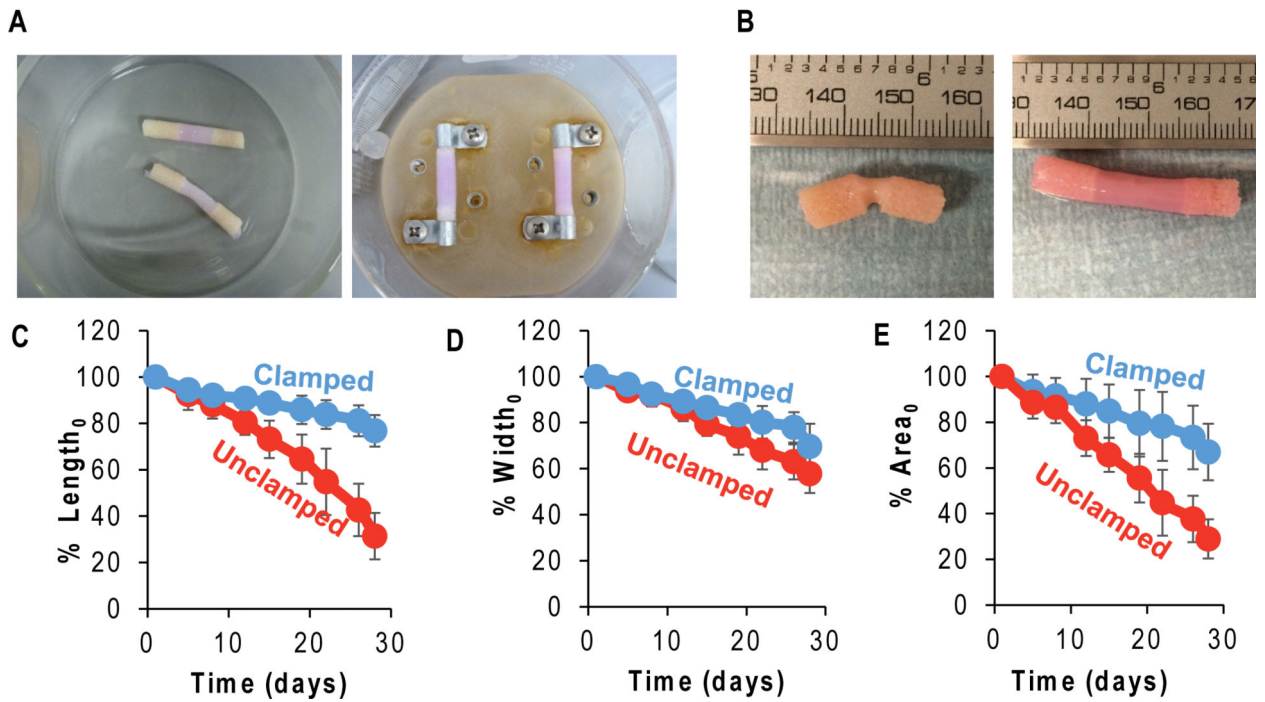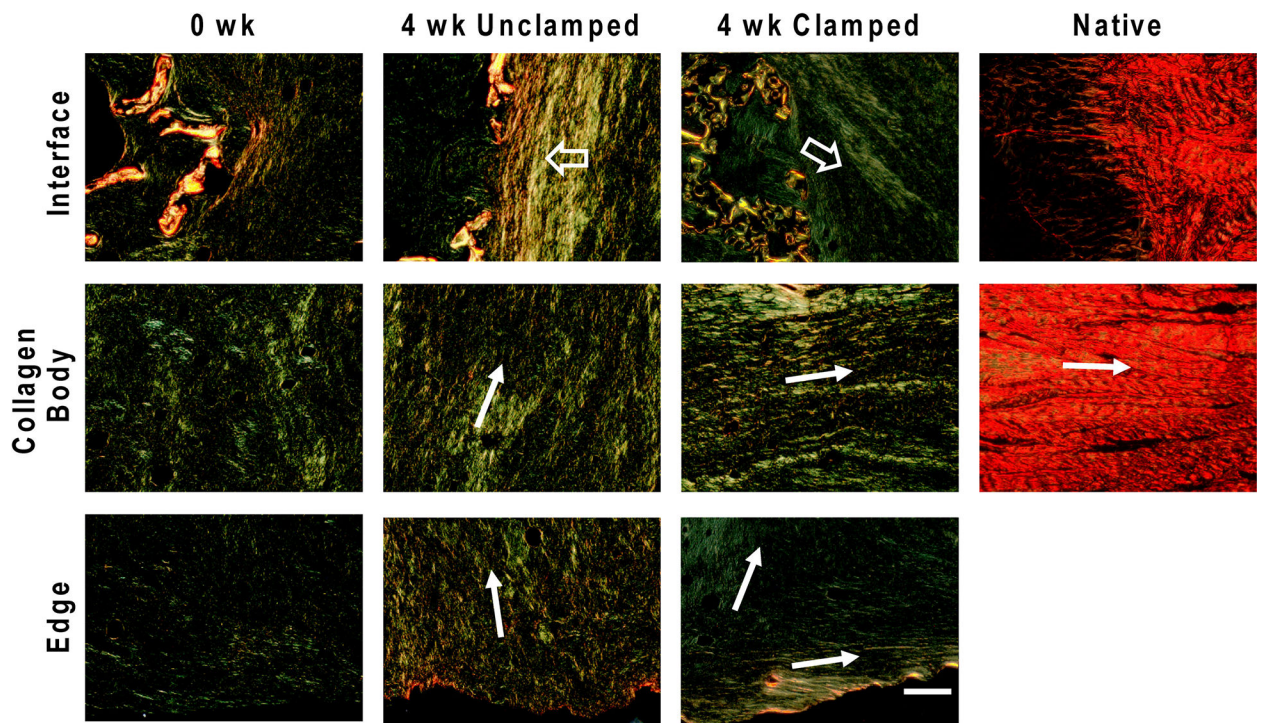
Figure 2:
(A) Top: 6 mm diameter bone cores from trabecular bone of bovine distal femur. Bottom: Deculluarlized bone cores using a hypotonic and detergent. (B) Bone plugs placed in to Tygon® tubing and clamped at each end (C) Collagen injection molded into Tygon® tubing. (D) Final construct with fiber direction axis labels. Fibers formed along the x-axis in the longitudinal direction or along the y-axis in the radial direction. Double sided arrows on the right indicate interface region where collagen penetrated into the trabecular bone.

Native Enthesis   **4 wk Clamped**

1 mm   1 mm

Figure 3:
(A) Unclamped (left) and clamped (right) enthesis culture set up. (B) Unclamped (left) and clamped (right) construct appearance after 4 week in culture. Projected length (C), width (D), and area (E) over time compared to initial measurements (significantly different with time and condition after 4 weeks or 28 days, $p<0.05$, n=7–8).

Figure 4:
Picrosirius red staining of soft tissue to bone interface of native left caudal meniscal enthesis (left) and 4 week clamped tissue engineered meniscal enthesis (right).
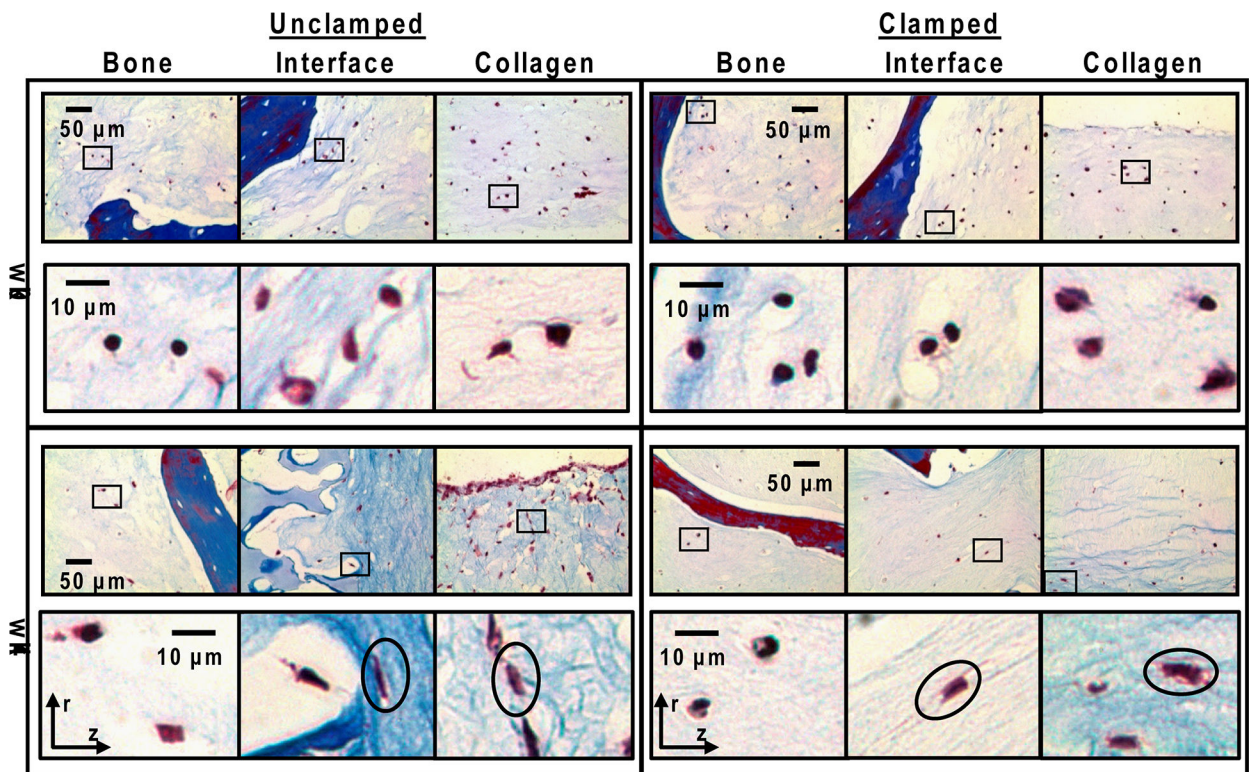
Figure 5:
Picrosirius red staining imaged using polarized light. 0 week generally disorganized collagen. Accordion compaction in 4 week unclamped versus integrated fibers at 4 week clamped interface (⇨). Fiber direction of collagen indicated by →.
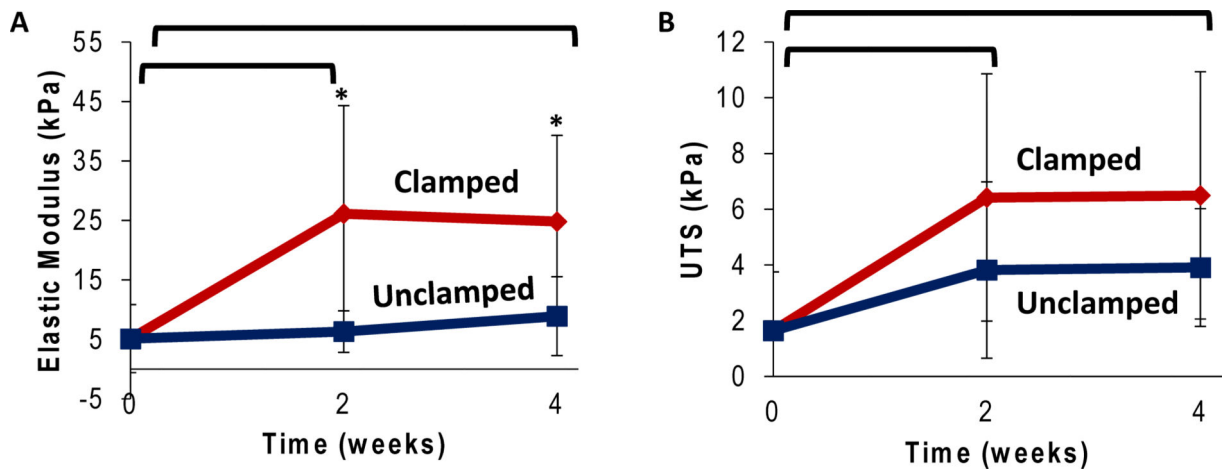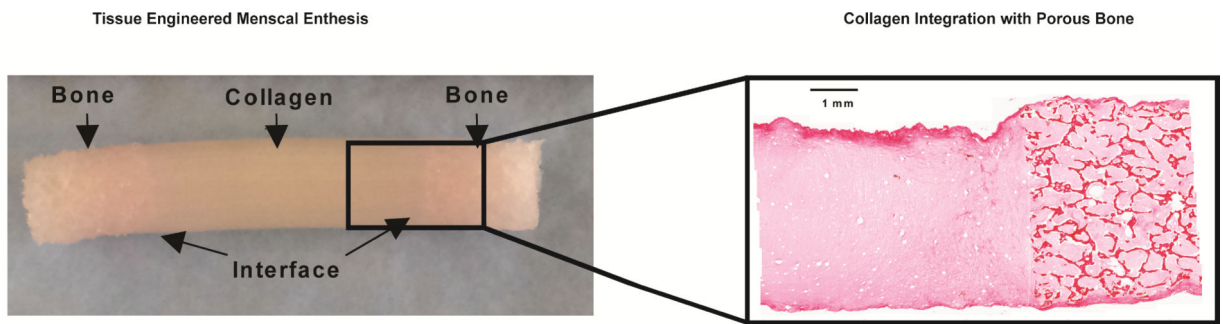
Figure 6:
Masson's Trichrome staining of cultured samples. Images taken from three areas of constructs: bone, interface, and collagen. Boxes indicate location of high magnification images in the row below. Circles indicate direction of cell elongation. Orientation of images relative to radial (r) and longitudinal (z) axis is shown by axis markers. Cell in bone region remain rounded while cells in the interface and collagen regions have a mix of rounded and elongated cells. Ovals in unclamped samples are aligned in the radial direction, while cells in clamped samples are aligned in the longitudinal direction.

Figure 7:
Tensile testing (.75% strain/sec) pull to failure testing to evaluate elastic modulus ($E_{Elastic}$) (A) and ultimate tensile strength (B) (* significantly different between conditions, ‒ significantly different over time, $p<0.05$, n=4–6).